

## Quasi-neutral simulations of tokamak scrape-off layer currents \*

V. Fuchs<sup>1</sup> and J. P. Gunn<sup>2</sup>

<sup>1</sup>Association EURATOM/IPP.CR, 18 200 Praha 8, Czech Republic

<sup>2</sup>Association EURATOM-CEA, CEA/DSM DRFC, Centre de Cadarache, 13108 Saint Paul lez Durance, France

**1 Introduction.** A fully kinetic quasi-neutral particle-in-cell (QPIC) code for tokamak plasma edge simulations was recently developed and successfully tested [1] against a well-known model of a Mach probe in a semi-infinite region (free presheath) with kinetic ions and Boltzmann electrons [2]. The present work is an extension of [1] to deal with tokamak scrape-off layer (SOL) plasma bounded by two solid targets (e.g. limiters, divertor plates, probes, etc.). The principal motivation for using a QPIC code in tokamak edge problems is the substantial reduction of the spatial Debye and temporal plasma period scales characteristic of standard PIC simulations. This is essential for simulations of large regions such as the SOL on an ion transit time scale. Furthermore, there are significant cases of interest where the electrons do not satisfy the Boltzmann assumption (adequate in [2]) thus requiring a fully kinetic treatment. Such, for example, is the case of supra-thermal electrons generated near a lower hybrid (LH) grill, or less obviously even that of electrons in a natural SOL of interest here, as is demonstrated in Fig 1. The electrons clearly require a sufficiently large region (typically  $L_p \cdot v_{the}/v_{thi}$ , where  $L_p$  is the characteristic pre-sheath parallel size) to equilibrate and, moreover, the highest energy electrons are being systematically removed by the targets.

We refer herein to three configurations of interest [3]: the natural SOL bounded by two solid targets, the connected presheath likewise bounded by two solid targets, but whose transverse dimension is determined by the targets rather than by balance between parallel (to  $\vec{B}$ ) and perpendicular flow as in the natural SOL, and the free presheath bounded by one solid target (typically a probe surface). The behaviour of the plasma in all three cases is principally determined by the sink action of the solid targets, which tend to absorb all incident ions. Equilibrium is established in particle balance between the sink and source effects, with the result that the natural SOL transverse dimension  $a_{\perp}$  adjusts so that the characteristic presheath length  $L_p = c_e a_{\perp}^2 / D_{\perp}$  equals the connection length,  $L_c = 2\pi q_a R_{maj}$ , between the targets. Here, the particle perpendicular diffusion coefficient is  $D_{\perp} \cong 1 \text{ m}^2/\text{s}$ ,  $c_e = \sqrt{q T_{e0}/m_i}$ ,  $T_{e0}$  is the source electron temperature and  $q_a$  is the tokamak edge safety factor. The ratio  $\lambda = L_c/L_p$  determines the nature of the two-wall configuration, such that the natural SOL at  $\lambda=1$  metamorphoses via the connected presheath for  $\lambda>1$  to the free

presheath as  $\lambda \rightarrow \infty$ . **Figure 1** shows that the plasma is not in equilibrium with the source term unless  $\lambda \rightarrow \infty$ . For low values of  $\lambda$  the wall sink effect is dominant suppressing the density to far below the source value  $n/n_0=1$ . This has an important effect on SOL quantities which depend on density, such as the SOL current and power-flow to the walls.

We first deal with the formulation of boundary conditions which adequately represent the effect of the material targets on the SOL plasma dynamics. Cases of interest are those with non-floating targets and asymmetric SOL configurations which both give rise to a non-zero SOL current. For illustration we show results for target biasing and the asymmetry originating from supra-thermal electrons generated near a LH grill. The code is validated under Mach probe conditions against known results [1,3,4] for background flow deduced from upstream-downstream ion current data.

**2 QPIC SOL boundary conditions.** A particular feature of the QPIC formalism is that it cannot describe the non-neutral sheath adjacent to a wall. Given the dominant sink effect of the sheath on the SOL plasma, the sheath has to be adequately represented by appropriate boundary conditions that particles reaching the walls have to satisfy. We modify here the “logical sheath” boundary condition of [5] to allow non-floating targets and a net current in the plasma. The basic condition is that all ions reaching the material targets are captured by the walls and neutralized by an appropriate number of most energetic electrons allowed to reach the walls, while all lower-energy electrons are reflected, respecting the condition of global charge conservation. In the one-wall –free presheath - problem, the wall therefore electrically floats. This is no longer necessarily true in the two-wall - SOL or connected presheath – configuration, where global charge conservation does not imply ambipolar flow to the walls. In general, the walls do not float when symmetry is broken: a net current flows from one wall to the other through the plasma. In either configuration the ion current is always saturated in the simulation, so the net current only depends on the electron current, which in turn depends on global charge conservation. The boundary conditions which must be satisfied at each time step of the QPIC simulation involve the wall potentials which, in turn, depend on distribution of wall charge and vice versa. The wall potentials are also tied together via a line integral  $\int_{\Gamma} \vec{E} \cdot d\vec{\ell} = 0$  along a loop  $\Gamma$  passing through the plasma and closing arbitrarily on a path outside the plasma but including possible electromotive forces, which give rise to a potential drop - a biasing voltage  $V_{\text{bias}}$ . We have, together with the requirement of global wall charge balance,

$$V_L + V_{pL} = V_R + V_{pR} \pm V_{\text{bias}}, \quad qw_{Li} + qw_{Ri} = qw_{Le} + qw_{Re} \quad (1)$$

where, for example,  $V_L$  and  $V_{pL}$  are respectively the wall and plasma potentials on the left, and the subscript Li refers to ions at the left target

The voltages in (1) are all negative with the given choice of reference potential  $\Phi(z_s)=0$  at the stagnation point  $z_s$  in the plasma. If we choose to bias the right wall negatively with respect to the left, then  $V_{\text{bias}} < 0$  comes with the sign (+). The individual wall net charge per time step is proportional to the current, which flows in the circuit. It is not necessarily zero, as would be the case for floating

walls. At each time step of the simulation we find a unique solution of Eqs (1) as the intersection of the potential arrays  $qV_{L,R} \approx -(1/2)m_e v_e^2$ . At each wall these arrays are made of  $Nq$  most energetic electrons, where  $Nq$  is the total wall ion charge. The solution are the wall potentials  $V_{L,R}$  and the corresponding wall charges (and thus also the SOL current).

**3 Selected results.** Any asymmetry around the SOL stagnation point introduced in the ion or electron properties will lead to a non-zero current. The most obvious such cases are background drift and biasing. In **Fig. 2a** we compare the computed drift velocity from ion wall currents [1-3] in the SOL configuration under  $L_c \gg L_p$  conditions, with the more usual free pre-sheath result, and in **Fig 2b** we show the corresponding SOL currents. **Figure 3** then shows the computed I-V characteristic in the biasing voltage range  $(-4, 4) [T_{e0}/q]$ . The given SOL configuration is clearly electrically equivalent to the double probe. As expected from the result of Fig.1, The theory prediction of Fig.3 (marked in blue), which is based on Boltzmann electrons, clearly fails for small values of  $\lambda=L_c/L_p$ .

Finally, we turn to the strongly non-Maxwellian case of suprathermal electrons generated in front of a lower hybrid grill [6-11]. Of particular interest is the associated heat flow toward target plates and a SOL current resulting from an asymmetrically phased grill. The grill is composed of 32 waveguides of width 1.05 cm with 90° directional phasing. The self-consistent electron velocity push [1] is here supplemented by a Langevin (Monte-Carlo) process describing electron velocity space diffusion in the LH grill spectrum [12]. In **Fig. 4** we give an example of power-flow driven by the Tore Supra LH grill electric field at  $E_0=1.0$  kV/cm. The increasing values of power-flow as a function of  $\lambda$  is caused by a concomitant increase in density as indicated by **Fig. 1**. The given computed values of power-flow are compatible with values measured on Tore Supra .

The ion powerflow, not shown here, is much smaller than the electron powerflow in the grill region. but is of the same order as the electron powerflow outside the grill where both electron and ion powerflows are driven by the self-consistent electric field. The thermal contribution to the total powerflow is about 40 %. To put the results of Fig.4 into perspective, we mention that in the absence of lower hybrid power, the electron powerflow is of the order of 0.06 MW/m<sup>2</sup>.

**4 Summary.** We have developed boundary conditions for the QPIC code in the general case of an asymmetric SOL bounded by two targets, and we have successfully tested the code in the cases of a drifting background, biasing and in the presence of supra-thermal electrons generated by a lower hybrid antenna electric field.

## References

\* Partly supported by the Czech Republic Grant Project GAČR 202/04/0360.

- 1 J. P. Gunn and V. Fuchs, Phys. Plasmas **14** (2007) 032501
- 2 K-S. Chung and I. H. Hutchinson, Phys. Rev. **A38** (1988) 472.
- 3 I. H. Hutchinson, Phys. Phys Fluids **B3** (1991) 847.
- 4 F. Valasque, G. Manfredi, J. P. Gunn, and E. Gauthier, Phys. Plasmas **9** (2002) 1806.

- 5 R. J. Procassini, C. K. Birdsall, and B. I. Cohen, Nuclear Fusion 30 (1990) 2329.
- 6 T. E. Evans, J. Neuhauser, F. Leuterer, et al. J. Nucl.Mater. **176-177** (1990) 202.
- 7 M. Goniche et al. *Acceleration of electrons in the near field of lower hybrid frequency grills*, Proc. 23<sup>rd</sup> European Conf. on Controlled Fusion and Plasma Heating, (Geneva: Kiev, European Physical Society) Vol. **20C**, (part II), pp783-786.
- 8 J. Mailloux et al., J. Nuclear Mater. **241-243** (1997) 745.
- 9 V. Fuchs, M. Goniche, Y. Demers, P. Jacquet, and J. Mailloux, Phys. Plasmas **3** (1996) 4023.
- 10 M. Goniche, et al., Nuclear Fusion **38** (1998) 919.
- 11 K. M. Rantamäki, T. J. H. Pättikangas, S. J. Karttunen, et al., Nucl. Fusion **40** (2000) 1477.
- 12 Fuchs, J. P. Gunn, M. Goniche, and V. Petržílka, Nucl. Fusion **43** (2003) 341.

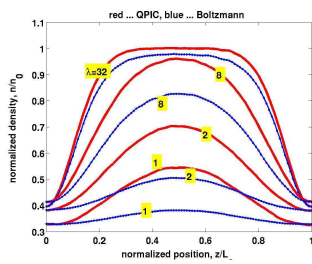


Fig. 1. SOL density profiles for different values of  $\lambda$ . Density is normalized to source density, distance to SOL connection length. Red curves correspond to fully kinetic electrons, blue curves to Boltzmann electrons.

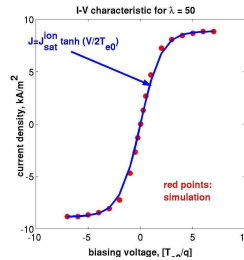
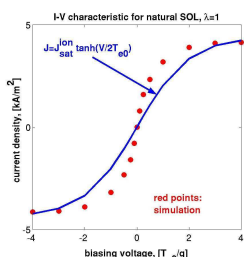


Fig. 3. Electric current flowing between targets through the SOL as a function of the applied voltage between the targets.

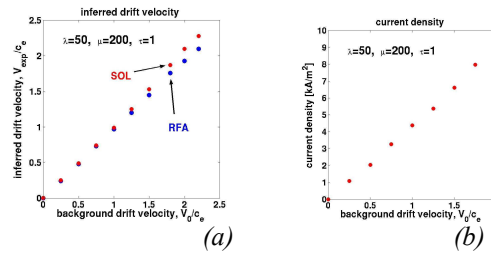


Fig. 2. (a) inferred plasma drift velocity obtained from ratio of ion currents to upstream and downstream targets, using Mach probe theory of Chung and Hutchinson. "SOL" corresponds to bounded plasma, "RFA" corresponds to semi-infinite plasma. Both results resolve fully kinetic electron distributions. (b) ion current density as a function of drift velocity.

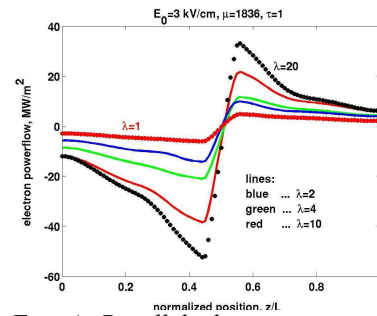


Fig. 4. Parallel electron power flow during local heating by a LH grill, for different values of  $\lambda$ . The grill is situated at the midpoint of the system. Main parameters are LH electric field  $E_0=3$  kV/cm, ion-to-electron mass ratio  $\mu=1836$ , and ion-to-electron temperature ratio  $\tau=1$ .